Proton Transfer in Carbonic Anhydrase Is Controlled by Electrostatics Rather than the Orientation of the Acceptor†

Demian Riccardi,‡ Peter König,§ Hua Guo,|| and Qiang Cui*,‡,§

Department of Chemistry and Program of Computation and Informatics in Biology and Medicine, University of Wisconsin, 1101 University Avenue, Madison, Wisconsin 53706, BACTER, University of Wisconsin, 433 Babcock Drive, Madison, Wisconsin 53706, and Department of Chemistry and Chemical Biology, University of New Mexico, Albuquerque, New Mexico 87131

Received September 26, 2007; Revised Manuscript Received November 20, 2007

ABSTRACT: Combined quantum mechanical/molecular mechanical (QM/MM) simulations are carried out to analyze factors that dictate the proton transfer in carbonic anhydrase II (CAII), an enzyme that has been used as a prototypical example of long-range proton transfers in biomolecules. In contrast to the long-held conjecture in the experimental literature, the computed potentials of mean force (PMF) suggest that the proton transfer in CAII is not very sensitive to the orientation of the acceptor group (His 64) and, therefore, the number of water molecules that bridge the donor (zinc−water) and acceptor groups. Perturbative analysis indicates that a series of polar and charged residues close to the transfer pathways make the dominant contribution to the barrier and exothermicity of the proton transfer reaction, thus supporting the proposal from previous studies of Warshel and co-workers using a somewhat simpler QM/MM model that electrostatic interactions play a major role in the proton transfer in CAII. The PMF results are in striking contrast to previous analysis using the same QM/MM method but an ensemble of minimum energy path (MEP) calculations, which found a steep dependence of the barrier height on the number of bridging water molecules. Analysis of the configurations sampled in the PMF and MEP simulations suggests that this difference arises because the PMF simulations sample a largely stepwise mechanism while the local MEP calculations artificially favored concerted transfers due to the specific protocol used to generate the initial configurations. Therefore, this study presents a compelling argument for carrying out proper conformational sampling in the study of long-range proton transfers. Finally, we illustrate that Φ analysis, which has been widely used in protein folding studies, can potentially generate new mechanistic information for long-range proton transfers regarding the sequence of events. The results of the perturbation analysis and the Φ analysis provide opportunities for experimentally testing the mechanistic proposals from this study and our recent work in which a stepwise "proton hole" transfer pathway has been proposed.

Proton transfers across a long distance are prevalent in biology, particularly in bioenergetics-related processes (*1*). The large number of protein residues and/or water molecules that potentially mediate the long-distance transfer makes the mechanistic analysis difficult using experiments alone. For example, mutations may perturb the water structure and modify the transfer pathway, which make it less straightforward to interpret the result in terms of establishing the role of specific residues in the wild-type enzyme. Reliable theoretical analyses can complement experimental studies by offering mechanistic insights, provided that the relevant structural, dynamic, and energetic characteristics of the system are all properly described (*2*−*5*). Here we report a theoretical analysis of the proton transfer in human carbonic anhydrase II (CAII)[1] using QM/MM simulations (*6*−*8*). Although this process has been treated as a prototypical model of long-range proton transfers in biology and therefore has been analyzed by many experimental (*9*, *10*) and theoretical studies (*11*−*23*), the fundamental microscopic factors that dictate the kinetics of the transfer remain controversial. In particular, it has long been believed that the proton transfer depends sensitively on the number of water molecules that bridge the donor (zinc-bound water) and acceptor groups (His 64) and, therefore, the orientation of the His 64 side chain (*24*, *25*). For example, the "out" configuration of His 64 observed in the X-ray structure (Figure 1) has been thought to be unproductive toward the proton transfer to or from the zinc site (*26*). In previous studies by Warshel and co-workers, who carefully analyzed the proton transfer kinetics in both the wild type and mutants of CAII (*11*−*13*) and CAIII (*14*, *15*) using the empirical valence bond-based methodology (*27*), the roles of electro-

† The studies were partially supported by the National Science Foundation (MCB-0314327, CHE-CAREER-0348649 to Q.C.) and the National Institutes of Health (R03AI068672 to H.G.). Q.C. is an Alfred P. Sloan Research Fellow.

* To whom the correspondence should be addressed. E-mail: cui@chem.wisc.edu. Phone: (608) 262-9801. Fax: (608) 262-4782.

‡ Department of Chemistry and Program of Computation and Informatics in Biology and Medicine, University of Wisconsin.

§ BACTER, University of Wisconsin.

|| University of New Mexico.

[1] Abbreviations: CAII, carbonic anhydrase II; GSBP, generalized solvent boundary potential; MEP, minimum energy path; PMF, potential of mean force; QM/MM, quantum mechanical/molecular mechanical; SCC-DFTB, self-consistent charge-density functional tight binding; WT, wild type.

10.1021/bi701950j CCC: $40.75
Published on Web 02/02/2008

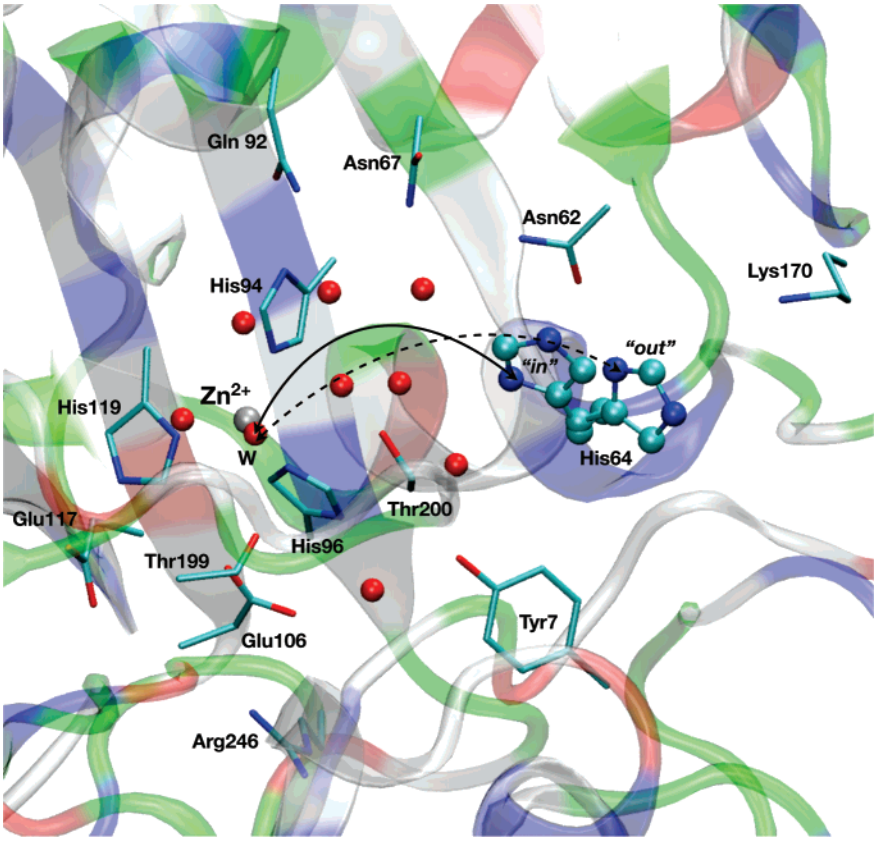

FIGURE 1: Active site of human carbonic anhydrase II based on the X-ray structure [PDB entry 2CBA (*52*)]. The proton transfer under study is between the zinc-bound water and His 64 (in ball-and-stick form), which has been resolved to adopt two orientations (in and out). A number of residues, which include the ligands of the zinc ion (His 94, His 96, and His 119) and those found to make significant contributions to the proton transfer energetics, are shown in line form. Water molecules within 7 Å of the zinc are shown as red spheres. The protein backbone is shown in ribbon form with the following color scheme: red for acidic, blue for basic, green for polar, and white for apolar.

static interactions and protein reorganization have been emphasized over the importance of acceptor orientation. However, the role of acceptor orientation has not been studied explicitly; it is entirely possible that the electrostatic environments of the "in" and out configurations of His 64 are substantially different and therefore lead to significantly different rates of proton transfer toward the acceptor.

In this work, we explicitly study the proton transfer energetics in CAII associated with different orientations of the acceptor group using potential of mean force (PMF) calculations and a calibrated QM/MM potential (*23*, *28*). The results suggest that acceptor orientation does not play a major role in CAII. Instead, supporting the view of Warshel and co-workers (*12*), perturbative analyses of the PMF results highlight the importance of specific electrostatic interactions along the transfer pathway, which is rather extensive in space. The striking difference between the PMF results and the findings from previous gas-phase model studies (*20*) and minimum energy path (MEP) calculations (*22*) emphasizes the importance of properly sampling the enzyme and solvent configurations in the study of long-range proton transfers. The current study also suggests that systematic Φ analysis (*29*) can be an interesting experimental approach that complements, for example, linear free energy analysis (*9*, *12*, *15*), for gaining additional insights into the mechanism of long-range proton transfers.

COMPUTATIONAL MODEL AND METHODS

The QM/MM simulations are carried out using the same SCC-DFTB (*30*)/MM-GSBP (*31*, *32*) protocol as described in details in ref *23* and therefore only summarized briefly. As discussed in recent studies (*22*, *33*), the self-consistent charge-density functional tight binding (SCC-DFTB) approach is a reasonable compromise between computational speed and accuracy, a feature that is crucial to a meaningful study of long-range proton transfer in biomolecules. For example, SCC-DFTB is sufficiently fast that on the order of 10 ns of sampling can be done for PMF simulations, which is substantially longer than most QM/MM simulations published to date (*8*, *34*, *35*). At the same time, the method is quite accurate for the potential energy surfaces of proton transfers involving the current donor, acceptor, and water molecules as compared to high-level (B3LYP, MP2 with triple-ζ plus polarization quality basis sets) QM calculations (see the Supporting Information). The solvation free energies of proton and hydroxide are two quantities that are crucial for a highly quantitative description of proton transfer reactions in the condensed phase but remain to be improved at the SCC-DFTB level (see discussions in ref *23*); we are making developments (*36*) with the goal of improving the description of these quantities in a systematic rather than an ad hoc manner. With regard to the boundary condition of the QM/MM simulations, previous simulations in our lab (*22*, *32*) have established that a careful treatment of

electrostatic interactions is crucial for preventing artificial side chain orientations and overflooding of the active site and that the generalized-solvent-boundary-condition (GSBP) protocol (*31*) is appropriate when the process of interest is far from the inner−outer boundary (*37*).

The SCC-DFTB region includes the zinc ion, its ligands, the His 64 side chain, and all water molecules in the active site between the donor and acceptor groups (10 and 22 for the in and out simulations, respectively); the QM waters are selected on the basis of two spheres centered on the zinc and His 64 Nδ, and thus, the number of waters in the QM region depends on the orientation of the acceptor. Using proton transfers between two 4-methylimidazole molecules in solution, it was established that the PMF is not very sensitive to the number of QM waters (see the Supporting Information of ref *23*). The H64A mutant is constructed in silico by changing His 64 to Ala. A water molecule tethered to a dummy atom with a harmonic spring is used as the proton acceptor in the H64A simulations, where the dummy atom is placed 12 Å from the zinc corresponding to the out configuration of His 64 in the WT enzyme; 24 water molecules are included in the SCC-DFTB region in the H64A simulations.

For the rest of the system, all atoms within 20 Å of the zinc are treated explicitly using the CHARMM22 force field (*38*) and form the inner region of the GSBP setup (*31*, *32*); more distant protein and water molecules are treated as the outer region on the basis of the Poisson−Boltzmann continuum electrostatics model. In the PMF simulations, a collective variable (ζ) based on the position of the "center of excess charge" relative to the proton donor (oxygen of zinc-bound water) and acceptor (e.g., Nδ of His 64 for the WT) is used as the reaction coordinate (*3*). As it varies from 0 to 1, this collective coordinate reports the migration of the center of excess charge from the donor to the acceptor. The use of a collective coordinate is crucial here because the configurations of water molecules that connect the donor and acceptor groups vary on the picosecond scale (*32*) and therefore should be properly averaged in the PMF simulations (*39*). Twenty windows are used for each system configuration (in and out for WT and one set for H64A) where each window typically lasts for 300 ps. To prevent the protonated His 64 from flipping out in the in set of simulations, a NOE restraint (with a force constant of 50 kcal mol^{-1} Å^{-2}) is applied to the CG atom of His 64 when it is more than 8.8 Å from the zinc atom. Note that the purpose of adding a restraint is to make it more transparent to compare the proton transfer energetics with those of the in and out His 64 configurations; due to the nature of the NOE restraint, the effect of the restraint is minimal when the His 64−zinc distance is below 8.8 Å, which is the case during the majority of the His 64 in simulations.

To help analyze the nature of the proton transfer configurations sampled in the current PMF and previous MEP (*22*) simulations, the "excessive coordination numbers" for the zinc-bound oxygen, His 64 Nδ, and oxygen in the intervening water molecules are calculated for the save configurations from these simulations. The excess coordination, $\nu_0^{X_i}$, of each heavy atom of interest, X_i, is determined using an expression introduced by Chakrabarti et al. (*40*):

$$\nu^{X_i} = \sum_{j=1}^{N_H} f_{sw}(d_{X_i,H_j}) - w^{X_i} \quad (1)$$

where $f_{sw}(d)$ and w^{X_i} are the same switching function and weight, respectively, used to define the center of excess charge (*23*); the coordination is normalized as follows

$$\nu_0^{X_i} = \frac{\nu^{X_i}}{\sum_{j=1}^{N_X} \nu^{X_j}} \quad (2)$$

This normalization enables the qualitative descriptor to determine how the protonation states vary in space, relative to the reaction coordinate. The parameters d_{sw} and r_{sw} are adjusted for optimum differentiation between hydroxide and hydronium geometries (r_{sw} = 1.25 Å and d_{sw} = 0.04 Å). For the position of the heavy atoms, we use an expression similar to ζ to measure the distance relative to the donor and acceptor atoms

$$\zeta_{X_i} = \frac{|\mathbf{r}^D - \mathbf{r}^{X_i}|}{|\mathbf{r}^D - \mathbf{r}^{X_i}| + |\mathbf{r}^A - \mathbf{r}^{X_i}|} \quad (3)$$

In short, the excess coordination number plots (Figure 3) report the variation of protonation states ($\nu_0^{X_i}$) for heavy atoms of interest as a function of the collective reaction coordinate (ζ) and the relative positions of the corresponding heavy atoms (ζ_{X_i}). For the classical Grotthuss mechanism, such a plot exhibits a diagonal feature; for the "proton-hole" mechanism (*23*), it exhibits an antidigonal feature, and for a concerted mechanism, it shows stripes of peaks perpendicular to the ζ axis and parallel to the ζ_{X_i} axis.

To estimate the contribution of a specific group to the PMF, a change in the mean force on the reaction coordinate is computed and integrated along the reaction coordinate when the partial charges on that group are set to zero. Such analysis is perturbative in nature because snapshots from the original PMF simulations (when all charges are present) are used. Compared to the similar analysis commonly conducted for MEP (*41*), the effects of thermal fluctuations are naturally included.

RESULTS AND DISCUSSION

PMFs for Two Different His 64 Orientations. As shown in Figure 2, the calculated PMF profile for the proton transfer between the zinc-bound water and His 64 is not very sensitive to the orientation of the His 64 side chain. Regardless of whether His 64 adopts the in or out configuration, the PMF is nearly thermoneutral and has a barrier around 12−13 kcal/mol. The thermoneutrality of the reaction is consistent with experimental kinetic measurements, which suggested that both the zinc-bound water and His 64 have a pK_a of 7 (*42*). The computed classical barrier of 12−13 kcal/mol is also consistent with the experimental rate constant that points to an apparent activation free energy barrier of ~10 kcal/mol (with the transition state theory, assuming a transmission coefficient of 1.0 and a prefactor of k_BT/h); previous studies (*8*, *13*, *43*) indicate that nuclear quantum effects for proton transfers in enzymes at 300 K have major contributions from

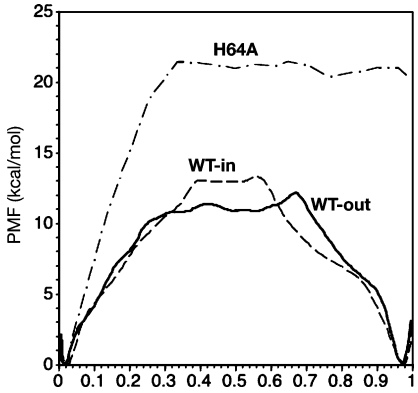

FIGURE 2: Calculated potential of mean force (PMF) for the proton transfer between the zinc-bound water and His 64 in the in and out configurations in WT CAII. Also shown is the PMF for the proton transfer in the H64A mutant from the zinc-bound water to a location at the protein−solvent interface that mimics the position of His 64 Nδ in WT CAII. The *x*-axis is a generalized coordinate (ζ) that characterizes the progress of the proton transfer (*3*, *23*).

zero-point energies, which typically reduce the barrier by 2−3 kcal/mol.

The PMF for the out configuration has a barrier similar to that of the in configuration, and the difference is comparable to the statistical uncertainty of the PMF calculations. What is clear, however, is that the out configuration is likely as productive for proton transfer as the in configuration, in contrast to the previous conjecture that the out configuration was unproductive at all for proton transfer (*10*, *26*). Analysis of the excess coordination number plots (*23*) (Figure 3) indicates that the proton transfers in both cases follow the proton-hole mechanism (*23*) in which the His 64 extracts a proton from the nearby water to form a hydroxide in the initial stage of the reaction, which then propagates toward the zinc-bound water. As shown in panels a and b of Figure 4, the transfer pathway spans a rather broad region in the active site.

Proton Transfer in H64A CAII. In our recent analysis of the proton-hole transfer versus the classical Grotthuss mechanism (*23*), we emphasized that the relative weight of the two mechanisms estimated by computations depends sensitively on the accuracy of the computational model, especially the treatment of interaction between hydronium or hydroxide and the protein or solvent environment and the intrinsic proton transfer energetics for the reactive moieties. Through carefully designed benchmark calculations in solution (*23*), we also showed that the SCC-DFTB/MM approach used here overestimates the solvation of hydroxide over hydronium, which therefore overestimates the weight of the proton-hole mechanism in CAII. Thus, it is important to demonstrate that the lack of distance dependence of the proton transfer observed in our PMF simulations is not unique to the proton-hole mechanism.

To this end, we study the proton transfer in the H64A mutant from the zinc-bound water to a location at the protein−solvent interface that is close to the position of His 64 Nδ in the out orientation in the WT enzyme; note that only the classical hydronium-based Grotthuss mechanism is possible for the H64A mutant (Figure 4c,d). The calculated PMF is uphill for small ζ (which is a collective variable that describes the progress of the proton transfer; see refs *3* and *23* for detailed discussions) and quickly reaches a plateau region for ζ beyond 0.3, as expected for a proton transfer without a high pK_a acceptor group. The barrier region is rather broad and ~21.4 kcal/mol above the reactant; thus, the apparent effect of mutation (21.4 − 13 = 8.4 kcal/mol) is overestimated by almost 7 kcal/mol versus experiment (20-fold slower than that of WT) (*44*). As discussed thoroughly in the benchmark calculations in ref *23*, we understand that this overestimation has contributions from both errors in proton affinity and solvation energy by the current SCC-DFTB/MM parametrization. Instead of constructing a system-dependent correction, we leave the result as is to emphasize that an accurate theoretical description of "delocalized" chemistry with a general QM/MM protocol remains an important challenge; efforts are being directed toward systematically improving the proton affinities and hydrogen bonding properties at the SCC-DFTB level in the condensed-phase setting (*36*). Most importantly, we note that the current study does not aim to argue, on the basis of the computed PMFs, that the proton hole is the dominant mechanism in CAII. The point is to illustrate that even with the classical Grotthus mechanism, there is only a weak dependence of the proton transfer energetics on the length of the water wire, as suggested by the shape of the calculated PMF.

PMF versus MEP Analysis. As shown in the previous simulations with either a classical model (*45*) or a QM/MM model (*16*, *22*, *32*), both the in and out His 64 configurations are correlated with water wires of diverse lengths that connect the zinc-bound water and His 64. Due to the longer distance from the zinc-bound water, the out configuration requires substantially longer water wires (four to six waters) than the in configuration (two or three waters) for proton transfers (*32*). Therefore, the fact that the two His 64 orientations have similar computed PMFs is in remarkable contrast to our previous analysis using extensive sets of local minimum energy path (MEP) calculations (*22*). In that study, the MEPs were collected from multiple simulations of three protonation states (CHOH, COHH, or "TS-reorganized" where the proton is delocalized across constrained water bridges with lengths of two, three, and four molecules). Essentially all the atoms were allowed to move in the MEP optimizations, but the inherently limited reorganization yielded reaction energetics that, on average, depended on the protonation state of the simulation. Insights into the largely static nature of the protein environment and the importance of water reorganization were gained. From the thermoneutral "TS-reorganized" results, the MEP barriers exhibited a steep dependence on the length of the water wire, increasing from 6.8 kcal/mol to 12.6 kcal/mol to 17.4 kcal/mol as the length of the bridge was increased from two to three to four molecules, respectively.

To emphasize the mechanistic difference between the PMF and MEP results, the excess coordination plots (*23*) from these simulations are compared in Figure 3. For the MEPs, the proton is transferred in a delocalized (concerted) fashion; for the PMF simulations, the plots indicate a stepwise process regardless of the proton-hole or Grotthuss transfer mechanism or the in or out orientation of His 64. Therefore, the steep distance dependence in the MEP results is likely an artifact of the concerted transfer process imposed by the specific protein/solvent configurations used as the initial configuration.

In a framework dominated by stepwise transfers, as shown schematically in Figure 5, the barrier is expected to be less

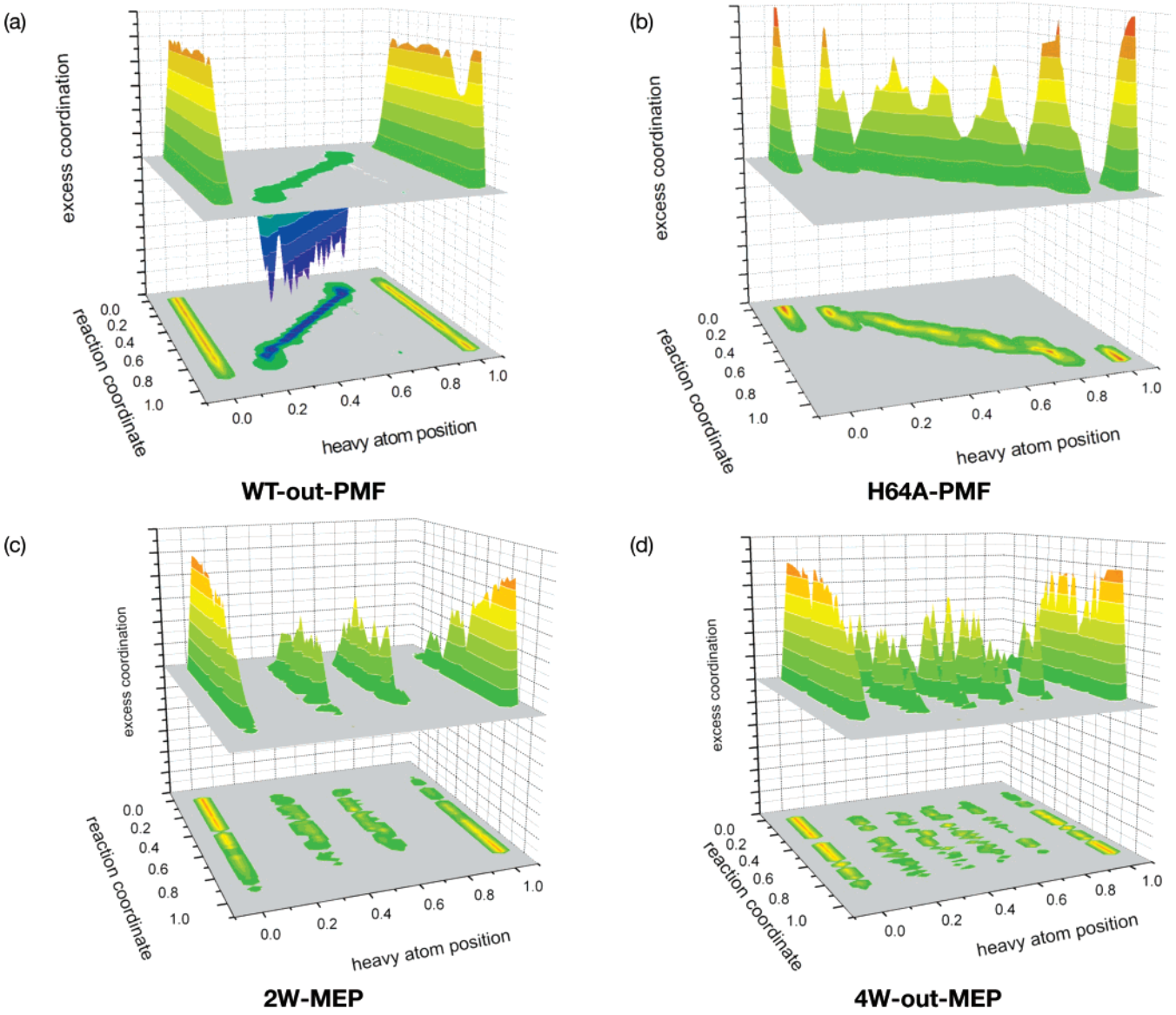

FIGURE 3: Excess coordination number plots (*23*) (see discussions of eqs 1−3 in the text) for different sets of PMF and MEP simulations. The patterns show that the WT PMF simulation follows the proton-hole mechanism, the H64A PMF simulation follows the classical Grotthuss mechanism, and the MEP calculations for the WT enzyme follow a very concerted mechanism.

sensitive to the length of the intervening wire (assuming the transfer is limited by thermal activation rather than diffusion of the hydronium/hydroxide), regardless of whether the microscopic process follows a classical Grotthuss mechanism or the proton-hole mechanism raised in our recent work. Here the barriers are largely correlated with the largest pK_a drop during the sequence of transfers. In CAII, since both the zinc-bound water and His 64 have a pK_a near 7.0, the rate-limiting step is expected to be either the proton transfer from the zinc-bound water to the active site waters or the proton-hole transfer from His 64 to the active site waters. The heterogeneous protein environment can shift the weights of these two pathways as well as the location of the transition state through electrostatic interactions [i.e., modifying the effective pK_a of water in the active site, as eloquently emphasized by Warshel and co-workers in their studies (*5*, *12*)].

It should be stressed that although the lack of distance dependence is obvious for a strictly stepwise mechanism, the insensitivity of the PMF to the His64 orientation is not a trivial result. First, the degree of "concertedness" for proton transfers in a realistic molecular environment cannot be predicted a priori, which is precisely the reason that the distance dependence of proton transfer in CAII has been a lingering debate despite many studies (*10*). Second, even in a framework where electrostatics play the major role, it is entirely possible that the in and out configurations of His 64 correspond to very different electrostatic environments and thus very different proton transfer rates. Therefore, evaluating the proton transfer energetics and kinetics for the in and out configurations of His 64 in a consistent manner has been an outstanding challenge to both experimental and theoretical studies.

Perturbative Analysis of Protein Contributions in WT CAII. To identify the protein residues that play an important role in controlling the energetics of the proton transfers in CAII, perturbative analysis is done for the PMFs on the basis of decomposing the residual contribution to the mean force along the approximate reaction coordinate (see Computational Model and Methods). As shown in Table 1, many polar and charged residues make notable contributions to both the

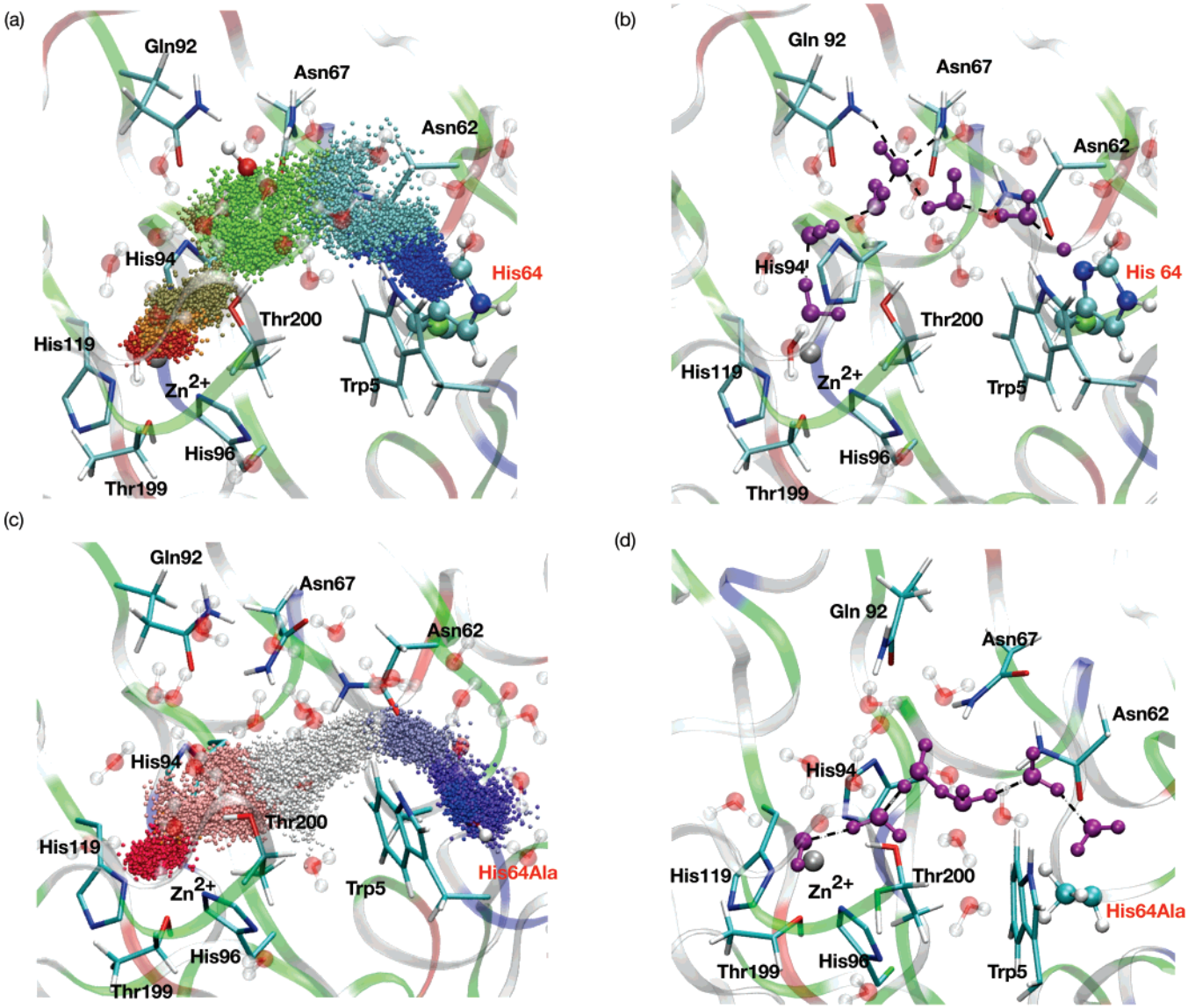

FIGURE 4: Locations of the center of excess charge (*3*) sampled in the PMF simulations for (a) WT and (c) H64A CAII, which illustrate the spatially broad transfer pathways associated with the proton transfers; different colors for the center of excess charge indicate sampling from different umbrella windows. (b and d) Snapshots from the transition state region (i.e., correspond to peaks in the computed PMFs) are shown to illustrate the local environment of (b) hydroxide in the WT and (d) hydronium in H64A simulations. The water wires that connect the zinc-bound water and His 64, including the hydroxide in the WT and hydronium in H64A, are colored purple.

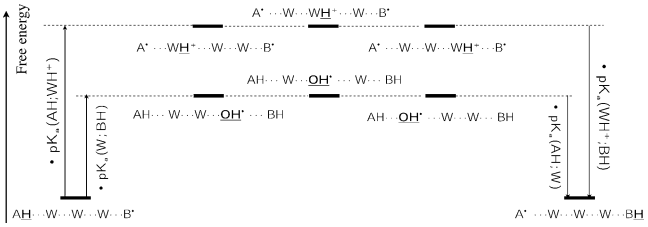

FIGURE 5: Schematics that illustrate the relative energetics of the Grotthus and proton-hole transfer mechanisms, which involve stepwise transfer of either hydroxide or hydronium ions. When pK_a differences are large, the basic energetic profile can be estimated on the basis of the pK_a values of the donor/acceptor groups (AH and BH) and water (W) as well as hydronium (WH^+), and the distance between the donor and acceptor is not an important factor (assuming that the process is not controlled by the diffusion of the hydronium or hydroxide).

reaction energy and barrier, some similar in spirit to the findings discussed in the studies of Warshel and co-workers (*11*, *14*, *15*). For the reaction energies, many of the same residues have been identified in our previous study to make a significant contribution to the pK_a of the zinc-bound water (*37*), although the magnitude is different, as expected. For example, two glutamates (Glu 106 and Glu 117) strongly disfavor the proton transfer from the zinc-bound water to His 64, while Arg 246 favors the process. Asn 62, a residue very close to His 64, favors the proton transfer, although it does not have a large impact on the zinc-bound water pK_a due to its charge neutrality and rather long distance from the zinc-bound water (Figure 1). Another residue, Lys 170, which is at the surface of CAII and spatially close to His 64 (Figure 1), disfavors the proton transfer to His 64, especially for the out orientation. Overall, the protein disfavors the proton transfer to His 64 by a significant amount, ~25.0 kcal/mol (see below).

For the barrier, the same set of residues makes major contributions. For some residues (e.g., Asn 62), the contribution to the barrier is almost the same as that to the reaction energy, and for others (e.g., Glu 106 and Glu 117), the contribution to barrier is nearly half of that to the reaction

Table 1: Contributions from Protein and Water to the Barrier and Reaction Energy (in kilocalories per mole) Associated with the Potential of Mean Force for the Proton Transfer from the Zinc-Bound Water in CAII[a]

perturbation[b]	distance (Å)[c]	WT-IN	WT-OUT	H64A[d]
exgr	−	1.1 (0.3)	0.8 (−0.7)	3.3 (2.9)
protein	−	27.4 (12.2)	28.8 (5.5)	27.0 (27.3)
water	−	−11.2 (−5.9)	0.2 (1.6)	−10.4 (−12.8)
T199	6.0	0.8 (−0.2) [−0.25/−0.25*]	−0.5 (−1.3) [2.6/2.2*]	0.3 (0.8) [/2.7*]
T200	7.2	1.5 (1.0) [0.67/0.60]	2.5 (1.9) [0.76/0.56]	1.0 (0.7) [/0.70]
L198	7.2	−2.1 (−1.7) [0.81/0.67]	−3.0 (−2.4) [0.80/0.50]	−1.3 (−0.8) [/0.62]
E117	7.6	10.8 (6.0) [0.56/0.47]	12.2 (6.0) [0.49/0.30]	10.4 (7.5) [/0.72]
E106	8.0	18.3 (9.4) [0.51/0.43]	23.7 (11.6) [0.49/0.19]	18.4 (13.5) [/0.73]
R246	9.1	−3.9 (−2.4) [0.62/0.51]	−5.4 (−3.3) [0.61/0.30]	−3.8 (−2.5) [/0.66]
N67	9.5	0.0 (−0.1) [−*]	−0.1 (−0.8) [−*]	−1.9 (−1.1) [/0.58]
Q92	10.1	2.0 (0.8) [0.40/0.30]	2.2 (0.5) [0.23/0.18]	1.2 (1.3) [/1.1*]
N62	12.5	−3.1 (−2.7) [0.87/0.84]	−4.9 (−5.4) [1.1/1.1*]	−3.4 (0.1) [/−0.0]
Y7	13.3	0.8 (0.1) [0.13/0.0]	2.4 (1.6) [0.67/0.33]	0.5 (0.0) [/0.0]
K170	16.9	7.7 (6.0) [0.78/0.70]	12.7 (10.5) [0.83/0.63]	9.2 (3.7) [/0.40]

[a] The results were obtained via charge perturbation analysis (see Computational Model and Methods). Contributions to the reaction free energy, $\Delta W^{pert}(\zeta\simeq1)$, and the barrier, $\Delta W^{pert}(\zeta_{TS})$, are shown without and with parentheses, respectively. The value in brackets is the Φ value (*29*) for each residue, defined as the $\Delta W^{pert}(\zeta_{TS})/\Delta W^{pert}(\zeta\simeq1)$ ratio; for the position of the transition state, both the WT PMF peak position (before slash) or simply $\zeta = 0.5$ (after slash) are used to explore the sensitivity of the estimated Φ values. Note that although Φ is expected to be between 0 and 1, the value can be out of this range when $\Delta W^{pert}(\zeta\simeq1)$ is close to be zero (indicated with an asterisk). [b] Labels correspond to the set of MM charges set to zero (both main chain and side chain atoms are included for a specific residue). [c] The distance is measured in the X-ray structure [PDB entry 2CBA (*52*)] between the corresponding Cα and the zinc ion. [d] The transition state is approximately set to $\zeta = 0.5$.

energy; in the language used for protein folding studies, this corresponds to Φ values (*29*) of 1 and 0.5, respectively. This difference reflects the fact that the interaction between the reactive moieties and some residues, such as Asn 62, is similar in the transition state and in the product state; for other residues such as Glu 106 and Glu 117, the interaction in the transition state is still substantially different from that in the product state. In the proton-hole mechanism sampled here, a negative charge migrates from His 64 toward the zinc-bound water; thus, it is expected that residues close to His 64 have high Φ values while those close to the zinc-bound water have low Φ values (see below).

Since a large number of water molecules are treated as QM, their contributions to the reaction are not readily revealed in the perturbative analysis. For waters in the MM region, the contribution is smaller, for both reaction energy and barrier, than that from the protein, especially for the out configuration. Previous analyses, however, indicated that water molecules undergo significant reorganizations (*46*) (reorientations) as the charge distribution of the active site changes during either proton transfer (*22*) or titration (*37*).

It is not straightforward to directly compare the perturbative results to available experimental mutation data because many mutations involve putting fairly large hydrophobic groups [Leu or Phe (*47*)] into or near the active site, which may significantly perturb the solvent structure and therefore transfer pathway. A more direct comparison can be made to a recent study in which Lys 170 has been mutated to an Ala or Glu, where the mutations were found to accelerate the proton transfer (D. N. Silverman, private communication). This is in qualitative agreement with the unfavorable contribution we found for Lys 170 in the WT enzyme; the very large magnitude of the result in Table 1 is due to the perturbative nature of the analysis, which has been shown to particularly overestimate the contribution of charged residues (*37*). The effect of Arg 246, which is not extremely close to the zinc-bound water but shown to be significant in Table 1, deserves further mutation studies.

Perturbative Analysis of Protein Contributions in H64A CAII. It is valuable to compare the protein contributions in H64A to those in WT CAII because any major difference might point to a way to experimentally distinguish the proton-hole mechanism from the Grotthuss mechanism in CAII. At the first glance (see Table 1), the result is somewhat disappointing in that the key residues make largely similar contributions in H64A as in WT CAII. For example, the major unfavorable contributions are from Glu 106, Glu 117, and Lys 170, while favorable contributions are from Asn 62 and Arg 246. This is not entirely surprising because the net flow of charges during the reaction is fairly similar in both the proton-hole (WT) and Grotthus (H64A) mechanisms.

A closer look, however, reveals interesting differences in the Φ values in the WT and H64A enzymes. For residues with significant contributions and spatially close to His 64, such as Asn 62 and Lys 170, the estimated Φ value is near 1.0 in the WT simulations; the values in the H64A mutant, by contrast, are much smaller. On the other hand, for those with significant contributions but spatially close to the zinc-bound water, such as Glu 106, Glu 117, and Gln 92, the estimated Φ values for the WT are close to or smaller than 0.5 while the corresponding values are substantially larger in the H64A mutant. These trends are consistent with the differences in the charge distribution of the reactive moieties in the proton-hole and Grotthus mechanisms. In the proton-hole mechanism, which is sampled in the WT simulations, the protonation state of His 64 and zinc-bound water in the transition state is similar to that in the product and reactant states, respectively; therefore, key residues close to His 64 are expected to have high Φ values while those close to the zinc-bound water low Φ values. By contrast, in the Grotthus mechanism, which is sampled in the H64A mutant simulations, the zinc-bound water is already deprotonated in the transition state. Therefore, key residues close to the zinc-bound water are expected to have high Φ values while those more distant have low Φ values. This realization suggests that by systematic mutation of key residues near the active site and analysis of the Φ values as functions of the distance to the donor/acceptor groups, it should be possible to reveal whether the proton-hole or the Grotthus mechanism is dominant in CAII! In other words, the Φ analysis is an

alternative way to correlate thermodynamic and kinetic data for proton transfer reactions compared to the linear free energy analysis. Although the latter can be formulated rigorously in terms of Marcus models, the interpretation depends on the number of diabatic states in the model (*9*, *15*).

CONCLUDING DISCUSSIONS

Long-range proton transfer reactions in biomolecules are fascinating because many factors potentially contribute to the determination of the kinetics and the underlying microscopic events. Revealing all the mechanistic details and pinning down the relative importance of various factors are tasks difficult to accomplish by experimental studies alone. Theoretical analysis can play a critical role, although a major challenge concerns how to distinguish new physical insights from artifacts caused by the approximate nature of computational techniques, a problem not dissimilar to the potential ambiguity in the interpretation of experimental results.

In this work, the issue of interest is whether the acceptor orientation and, therefore, the length of the mediating water wire are likely important limiting factors for the proton transfer in CAII. This is not a trivial issue because the competition between "concerted" and "stepwise" proton transfers cannot be predicted a priori in a realistic molecular environment and the different acceptor orientations may correspond to rather different electrostatic environments. We analyze these mechanistic issues using an efficient QM/MM approach that has been carefully analyzed by various applications (*22*, *48*) and benchmark studies (also see the Supporting Information). Although systematic errors in the QM/MM method remain, which we do not attempt to conceal using system-dependent "corrections", the method is sufficient for the current purpose of studying the wire length dependence of the proton transfer in CAII (see below).

The PMF simulations that used a flexible collective variable as the reaction coordinate sampled stepwise transfers in both the proton-hole and Grotthus pathways; note that there is no intrinsic bias toward a stepwise mechanism by the collective coordinate. Therefore, the height and position of the barrier are largely determined by the electrostatic interactions in the active site, which modulate the effective pK_a of the water molecules and the donor/acceptor groups, as confirmed by perturbative analysis of the mean forces along the reaction coordinate. The length of the mediating water wire does not come into the picture as an important factor. The qualitative difference between the PMF and the recent MEP results (*22*), especially concerning the energetics for the proton transfer to the out configuration of His 64, once again highlights the importance of carrying out extensive and proper sampling for long-range proton transfers. These conclusions are largely consistent with the findings of Warshel and co-workers, who have emphasized the importance of electrostatics in CAII and were able to reproduce a significant body of experimental data (*11*, *12*, *14*, *15*). The major differences lie in the less-system-specific QM/MM protocol used in our study, the explicit comparison of proton transfer energetics for the different acceptor orientations, and different ways of analyzing the protein contributions.

It is important to discuss these findings in the context of available experimental studies that have been interpreted to support the distance dependence of proton transfer in CAII. In the study of Fisher et al. (*25*), double mutants H64A/N62H and H64A/N67H were constructed and the proton transfer rates were measured. It was found that the H64A/N67H mutant is more effective than H64A/N62H for proton transfer by nearly 1 order of magnitude. The crystal structures of these mutants revealed that while His67 is connected to the zinc-bound water via two water molecules, His 62 is at least three water molecules from the zinc-bound water. The result was interpreted to suggest that the length of the water wire is responsible for the difference in the proton transfer rates in the two mutants. However, a closer inspection of the two active sites suggests that His 62 is involved in hydrogen bonding interactions with both of its nitrogen atoms and therefore is not in a position to accept a proton. Therefore, the proton transfer rate in H64A/N62H is expected to be similar to that in H64A, which is indeed consistent with the experimental measurement (*25*). An explicit computational analysis of the two double mutants is of great interest and being carried out. We note that this is not a trivial computational study since the proton transfer pathway in H64A/N62H, as argued above, may not be clearly defined.

Another key experimental observation that has been used to argue that the out configuration of His 64 is unproductive for proton transfer is based on combined mutation and small molecule rescue studies (*26*). It has long been established that small molecules such as 4-methylimidazole (4-MI) can enhance the proton transfer rate in H64A to the same level as that of WT CAII (*44*). An X-ray structure has captured the binding of 4-MI near Trp 5 through π-stacking interactions (*49*). Mutation of Trp 5 to Ala, Leu, or Phe had no significant impact on the rescue effect of 4-MI, which led to the conclusion that the observed binding site is unproductive toward proton transfer (*26*). Since this binding site of 4-MI closely mimics the position of His 64 in the out configuration, it was inferred that the out configuration of His 64 must be unproductive toward proton transfer as well. In our opinion, this interpretation is not unique. The lack of change in the rescue effect of 4-MI can be due to the existence of multiple binding sites, which may, in fact, suggest that the rescue ability of 4-MI is not very sensitive to the distance separation from the proton donor.

In short, we believe that although those experimental studies are highly instructive, the observations have alternative explanations that in fact underline the importance of electrostatic interactions in the active site rather than the length of the water bridge. Although the validity of the mechanistic proposals in our studies needs to be further examined by more extensive comparisons between computations and experiments, we note that the rate-limiting proton transfer in CAII is not dramatically accelerated on the basis of pK_a considerations; i.e., the proton transfer rate is not very different from the expectation based on pK_a values of the donor, acceptor groups, and water, and thus, the pressure to "fine-tune" the proton transfer rate is not great. The real evolution pressure seems to be maintaining similar pK_a values for the zinc-bound water and His 64, as reflected by the significant protein contributions to increase the pK_a of the zinc-bound water (*37*), such that the enzyme can work with a similar efficiency in both the hydration and dehydration directions. Along this line, although pK_a is intrinsically a thermodynamic parameter, revealing factors that control the

pK_a values of essential groups is an important step toward understanding proton transfers, as emphasized by us (*37*) and particularly by Warshel (*5*, *46*, *50*).

Finally, we emphasize that the flexibility of the QM/MM framework has been essential for revealing the potential importance of the proton-hole pathway (*23*). The systematic errors in the QM/MM potential energies are expected to be less significant in the discussion of relative quantities such as the importance of a residue or length of the water wire. In the current context, the most severe issue is that the solvation free energies of proton and hydroxide are not described well at the current SCC-DFTB level, which may overemphasize the importance of the proton-hole mechanism over the classical Grotthuss mechanism in CAII (*23*). One may argue that the overstabilization of hydroxide may also artificially favor a stepwise over a more concerted pathway in the PMF simulations and thus underestimates the distance dependence of the proton transfer. Although this remains a possibility, we note that the PMF also quickly reaches a plateau in the H64A simulations where the mechanism is the proton-based Grotthuss mechanism. Nevertheless, it is crucial to further improve the description for the potential energy function of proton transfers (*36*) and to go beyond the equilibrium analysis performed here using activated dynamics or transition path sampling (*51*). Ultimately, all computational predictions have to be verified by experimental studies; along this line, we believe that the Φ analysis can be an interesting way to complement other popular approaches such as the linear free energy analysis (*9*, *12*, *15*) to glean new mechanistic information for long-range proton transfers in complex systems.

ACKNOWLEDGMENT

Assistance from N. Ghosh and D. Xu in the early stage of the project is acknowledged. Computational resources from the National Center for Supercomputing Applications at the University of Illinois are greatly appreciated.

SUPPORTING INFORMATION AVAILABLE

Additional benchmark studies that support the use of SCC-DFTB for probing proton transfers in carbonic anhydrase based on gas-phase model calculations at both the B3LYP and MP2 levels. This material is available free of charge via the Internet at http://pubs.acs.org.

REFERENCES

1. Nicholls, D. G., and Ferguson, S. J. (2002) *Bioenergetics*, Vol. 3, Academic Press, New York.
2. Roux, B. (2002) Computational studies of the gramicidin channel, *Acc. Chem. Res. 35*, 366−375.
3. Koenig, P., Ghosh, N., Hoffman, M., Elstner, M., Tajkhorshid, E., Frauenheim, T., and Cui, Q. (2006) Towards theoretical analysis of long-range proton transfer kinetics in biomolecular pumps, *J. Phys. Chem. A 110*, 548−563.
4. Voth, G. A. (2006) Computer simulation of proton solvation and transport in aqueous and biomolecular systems, *Acc. Chem. Res. 39*, 143−150.
5. Kato, M., Pisliakov, A. V., and Warshel, A. (2006) The barrier for proton transport in aqauporins as a challenge for electrostatic models: The role of protein relaxation in mutational calculations, *Proteins: Struct., Funct., Bioinf. 64*, 829−844.
6. Warshel, A., and Levitt, M. (1976) Theoretical studies of enzymic reactions: Dielectric, electrostatic and steric stabilization of carbonium-ion in reaction of lysozyme, *J. Mol. Biol. 103*, 227−249.
7. Field, M. J., Bash, P. A., and Karplus, M. (1990) A combined quantum mechanical and molecular mechanical potential for molecular dynamics simulations, *J. Comput. Chem. 11* (6), 700−733.
8. Gao, J., and Truhlar, D. G. (2002) Quantum mechanical methods for enzyme kinetics, *Annu. Rev. Phys. Chem. 53*, 467.
9. Silverman, D. N. (2000) Marcus rate theory applied to enzymatic proton transfer, *Biochim. Biophys. Acta 1458*, 88−103.
10. Silverman, D. N., and McKenna, R. (2007) Solvent mediated proton transfer in catalysis by carbonic anhydrase, *Acc. Chem. Res. 40*, 669−675.
11. Åqvist, J., and Warshel, A. (1992) Computer simulation of the initial proton transfer step in human carbonic anhydrase, *J. Mol. Biol. 224*, 7−14.
12. Warshel, A., Hwang, J. K., and Åqvist, J. A. (1992) Computer-simulations of enzymatic-reactions: Examination of linear free-energy relationships and quantum-mechanical corrections in the initial proton-transfer step of carbonic-anhydrase, *Faraday Discuss. 93*, 225−238.
13. Hwang, J. K., and Warshel, A. (1996) How important are quantum mechanical nuclear motions in enzyme catalysis, *J. Am. Chem. Soc. 118*, 11745−11751.
14. Braun-Sand, S., Strajbl, M., and Warshel, A. (2004) Studies of proton translocations in biological systems: Simulating proton transport in carbonic anhydrase by evb-based models, *Biophys. J. 87*, 2221−2239.
15. Schutz, C. N., and Warshel, A. (2004) Analyzing free energy relationships for proton translocations in enzymes: Carbonic anhydrase revisited, *J. Phys. Chem. B 108*, 2066−2075.
16. Toba, S., Colombo, G., and Merz, K. M. J. (1999) Solvent dynamics and mechanism of proton transfer in human carbonic anhydrase II, *J. Am. Chem. Soc. 121*, 2290−2302.
17. Lu, D. S., and Voth, G. A. (1998) Proton transfer in the enzyme carbonic anhydrase: An ab initio study, *J. Am. Chem. Soc. 120*, 4006−4014.
18. Fisher, S. Z., Maupin, C. M. M., Budayova-Spano, L., Govindasamy, C., Tu, M., Agbandje-McKenna, D. N., Silverman, G., Voth, A., and McKenna, R. (2007) Atomic crystal and molecular dynamics simulation structures of human carbonic anhydrase II: Insights into the proton transfer mechanism, *Biochemistry 46*, 2930−2937.
19. Maupin, C. M., and Voth, G. A. (2007) Preferred orientations of His64 in human carbonic anhydrase II, *Biochemistry 46*, 2938−2947.
20. Cui, Q., and Karplus, M. (2003) Is "proton wire" concerted or step-wise? A model study of proton transfers in carbonic anhydrase, *J. Phys. Chem. B 107*, 1071−1078.
21. Smedarchina, Z., Siebrand, W., Fernandez-Ramos, A., and Cui, Q. (2003) Kinetic isotope effects for concerted multiple proton transfer: A direct dynamics study of an active site model of carbonic anhydrase II, *J. Am. Chem. Soc. 125*, 243−251.
22. Riccardi, D., Schaefer, P., Yang, Y., Yu, H., Ghosh, N., Prat-Resina, X., Konig, P., Li, G., Xu, D., Guo, H., Elstner, M., and Cui, Q. (2006) Development of effective quantum mechanical/molecular mechanical (QM/MM) methods for complex biological processes, *J. Phys. Chem. B 110*, 6458−6469.
23. Riccardi, D., König, P., Prat-Resina, X., Yu, H., Elstner, M., Frauenheim, T., and Cui, Q. (2006) "Proton holes" in long-range proton transfer reactions in solution and enzymes: A theoretical analysis, *J. Am. Chem. Soc. 128*, 16302−16311.
24. Silverman, D. N. (1995) Proton transfer in carbonic anhydrase measured by equilibrium isotope exchange, *Methods Enzymol. 249*, 479−503.
25. Fisher, Z., Hernandez Prada, J. A., Tu, C., Duda, D., Yoshioka, C., Govindasamy, A. H. L., Silverman, D. N., and McKenna, R. (2005) Structural and kinetic characterization of active-site histidine as a proton shuttle in catalysis by human carbonic anhydrase II, *Biochemistry 44*, 1097−1105.
26. An, H., Tu, C., Duda, D., Montanez-Clemente, I., Math, K., Laipis, P. J., McKenna, R., and Silverman, D. N. (2002) Chemical rescue in catalysis by human carbonic anhydrase II and III, *Biochemistry 41*, 3235−3242.
27. Warshel, A. (1991) *Computer Modeling of Chemical Reactions in Enzymes and Solution*, Wiley, New York.
28. Cui, Q., Elstner, M., Kaxiras, E., Frauenheim, T., and Karplus, M. (2001) A QM/MM implementation of the self consistent charge density functional tight binding (SCC-DFTB) method, *J. Phys. Chem. B 105* (2), 569−585.

29. Matouschek, A., Kellis, J. T., Serrano, L., and Fersht, A. R. (1989) Mapping the transition state and pathway of protein folding by protein engineering, *Nature 340*, 122.
30. Elstner, M., Porezag, D., Jungnickel, G., Elstner, J., Haugk, M., Frauenheim, T., Suhai, S., and Seifert, G. (1998) Self-consistent-charge density-functional tight-binding method for simulations of complex materials properties, *Phys. Rev. B 58* (11), 7260−7268.
31. Im, W., Bernéche, S., and Roux, B. (2001) Generalized solvent boundary potential for computer simulations, *J. Chem. Phys. 114* (7), 2924−2937.
32. Schaefer, P., Riccardi, D., and Cui, Q. (2005) Reliable treatment of electrostatics in combined QM/MM simulation of macromolecules, *J. Chem. Phys. 123*, 014905.
33. Elstner, M. (2006) The SCC-DFTB method and its application to biological systems, *Theor. Chim. Acta 116*, 316−325.
34. Friesner, R. A., and Guallar, V. (2005) Ab initio QM and QM/MM methods for studying enzyme catalysis, *Annu. Rev. Phys. Chem. 56*, 389−427.
35. Senn, H. M., and Thiel, W. (2007) QM/MM methods for biological systems, *Top. Curr. Chem. 268*, 173−290.
36. Yang, Y., Yu, H., York, D., Cui, Q., and Elstner, M. (2007) Extension of the self-consistent-charge tight-binding-density-functional (SCC-DFTB) method: Third order expansion of the DFT total energy and introduction of a modified effective coulomb interaction, *J. Phys. Chem. A 111*, 10861−10873.
37. Riccardi, D., and Cui, Q. (2007) pK_a analysis for the zinc-bound water in human carbonic anhydrase II: Benchmark for "multi-scale" QM/MM simulations and mechanistic implications, *J. Phys. Chem. A 111*, 5703−5711.
38. MacKerell, A. D., Jr., Bashford, D., Bellot, M., Dunbrack, R. L., Jr., Evanseck, J. D., Field, M. J., Fischer, S., Gao, J., Guo, H., Ha, S., Joseph-McCarthy, D., Kuchnir, L., Kuczera, K., Lau, F. T. K., Mattos, C., Michnick, S., Ngo, T., Nguyen, D. T., Prodhom, B., Reiher, W. E., III, Roux, B., Schlenkrich, M., Smith, J., Stote, R., Straub, J., Watanabe, M., Wiorkiewicz-Kuczera, J., Yin, D., and Karplus, M. (1998) All-atom empirical potential for molecular modeling and dynamics studies of proteins, *J. Phys. Chem. B 102*, 3586−3616.
39. Berezhkovskii, A. M., Szabo, A., Weiss, G. H., and Zhou, H. X. (1999) Reaction dynamics on a thermally fluctuating potential, *J. Chem. Phys. 111*, 9952−9957.
40. Chakrabarti, N., Tajkhorshid, E., Roux, B., and Pomès, R. (2004) Molecular basis of proton blockage in aquaporins, *Structure 12*, 65.
41. Cui, Q., and Karplus, M. (2003) Catalysis and specificity in enzymes: A study of triosephosphate isomerase (tim) and comparison with methylglyoxal synthase (mgs), *Adv. Protein Chem. 66*, 315−372.
42. Silverman, D. N., and Lindskog, S. (1988) The catalytic mechanism of carbonic anhydrase: Implications of a rate-limiting protolysis of water, *Acc. Chem. Res. 21*, 30−36.
43. Cui, Q., and Karplus, M. (2002) Quantum mechanics/molecular mechanics studies of triosephosphate isomerase-catalyzed reactions: Effect of geometry and tunneling on protontransfer rate constants, *J. Am. Chem. Soc. 124*, 3093−3124.
44. Tu, C., Silverman, D. N., Forsman, C., Jonsson, B., and Lindskog, S. (1989) Role of histidine 64 in the catalytic mechanism of human carbonic anhydrase II studied with a site-specific mutant, *Biochemistry 28*, 7913−7918.
45. Lu, D., and Voth, G. A. (1998) Molecular dynamics simulations of human carbonic anhydrase II: Insight into experimental results and the role of solvation, *Proteins: Struct., Funct., Genet. 33*, 119−134.
46. Warshel, A. (2003) Computer simulations of enzyme catalysis: Methods, progress and insights, *Annu. Rev. Biophys. Biomol. Struct. 32*, 425−443.
47. Fisher, S. Z., Tu, C., Bhatt, D., Govindasamy, L., Agbandje-McKenna, M., McKenna, R., and Silverman, D. N. (2007) Speeding up proton transfer in a fast enzyme: Kinetic and crystallographic studies on the effect of hydrophobic amino acid substitutions in the active site of human carbonic anhydrase II, *Biochemistry 46*, 3803−3813.
48. Elstner, M., Frauenheim, T., and Suhai, S. (2003) An approximate DFT method for QM/MM simulations of biological structures and processes, *THEOCHEM 632*, 29.
49. Duda, D., Tu, C., Qian, M., Laipis, P. J., Agbandje-McKenna, M., Silverman, D. N., and McKenna, R. (2001) Structural and kinetic analysis of the chemical rescue of the proton transfer function of carbonic anhydase II, *Biochemistry 40*, 1741−1748.
50. Warshel, A., and Ålqvist, J. A. (1991) Electrostatic energy and macromolecular function, *Annu. Rev. Biophys. Biophys. Chem. 20*, 267−298.
51. Bolhuis, P. G., Chandler, D., Dellago, C., and Geissler, P. L. (2002) Transition path sampling: Throwing ropes over rough mountain passes, in the dark, *Annu. Rev. Phys. Chem. 3*, 291−318.
52. Håkansson, K., Carlsson, M., Svensson, L. A., and Liljas, A. (1992) Structure of native and apo carbonic anhydrase II and structure of some its anion-ligand complexes, *J. Mol. Biol. 227*, 1192−1204.

BI701950J